Featured in Physics

Probing Curved Spacetime with a Distributed Atomic Processor Clock

Jacob P. Covey,[1,*] Igor Pikovski,[2,3,†] and Johannes Borregaard[4,‡]

[1] *Department of Physics, The University of Illinois at Urbana-Champaign, Urbana, Illinois 61801, USA*
[2] *Department of Physics, Stockholm University, SE-106 91 Stockholm, Sweden*
[3] *Department of Physics, Stevens Institute of Technology, Hoboken, New Jersey 07030, USA*
[4] *Department of Physics, Harvard University, Cambridge, Massachusetts 02138, USA*

(Received 24 February 2025; accepted 22 May 2025; published 21 July 2025)

Quantum dynamics on curved spacetime has never been directly probed beyond the Newtonian limit. Although we can describe such dynamics theoretically, experiments would provide empirical evidence that quantum theory holds even in this extreme limit. The practical challenge is the minute spacetime curvature difference over the length scale of the typical extent of quantum effects. Here, we propose a quantum network of alkaline earth (like) atomic processors for constructing a distributed quantum state that is sensitive to the differential proper time between its constituent atomic processor nodes, implementing a quantum observable that is affected by post-Newtonian curved spacetime. Conceptually, we propose to delocalize one clock between three locations by encoding the presence or absence of a clock into the state of the local atoms. By separating three atomic nodes over approximately kilometer-scale elevation differences and distributing one clock between them via a W state, we demonstrate that the curvature of spacetime is manifest in the interference of the three different proper times that give rise to three distinct beat notes in our nonlocal observable. We further demonstrate that N-atom entanglement within each node enhances the interrogation bandwidth by a factor of N. We discuss how our proposed system can probe new facets of fundamental physics, such as the linearity, unitarity, and probabilistic nature of quantum theory on curved spacetime. Our protocol combines several recent advances with neutral atom and trapped ions to realize a novel quantum probe of gravity uniquely enabled by quantum networks.

DOI: 10.1103/q188-b1cr

I. INTRODUCTION

The interface between quantum theory and gravity remains elusive. There are two main manifestations of this interface: the quantization of the gravitational field itself [1] and the dynamics of quantum systems on a classical curved spacetime [2]. Despite recent ideas on detecting quantum features of gravity with novel quantum systems [3–7], their experimental implementation remains a significant challenge. In contrast, detecting the influence of curved spacetime on quantum systems only requires quantum mechanical probes. The effect of Earth's gravity in the dynamics of quantum systems can be readily observed. But so far, this has only been achieved in the Newtonian limit, such as in matter-wave interferometry [8,9], where Newtonian gravity induces a coherent phase shift, or in neutron-bouncing experiments [10,11], where the Newtonian potential acts as a potential well for neutrons. Going beyond the Newtonian limit, and observing genuine quantum phenomena affected by curved spacetime, remains a challenge. While post-Newtonian corrections to the potential can result in modifications of the phase shift [12], there are also effects unique to gravity, such as gravitational time dilation, which result in different signatures in the quantum domain.

One such effect is the loss and revival of coherence due to gravitational time dilation, for which both quantum theory and general relativity (GR) have to be taken into account [13]. This can be achieved through quantum interference of clocks that experience different proper times in superposition [13,14]. One prepares internal states in superposition, such as a qubit, and also separates the system into a superposition of two or more distant locations. The time dilation induced by Earth's gravitational field will cause the delocalized clock qubit to evolve

*Contact author: jcovey@illinois.edu
†Contact author: pikovski@stevens.edu
‡Contact author: borregaard@fas.harvard.edu

differently in the two positions. This results in a periodic loss and revival of the visibility of interferometric "self-interference" measurements as a signature of the interplay of quantum dynamics and general relativistic proper time evolution [13,15–20]. While the predictions have been simulated with BECs in a magnetic field [21], the experiment in Earth's gravitational field remains challenging due to the required separations and coherence times: to see full loss and revival, one needs a spatial superposition on the order of 10 m and coherence of 1 s, in addition to the preparation of both internal and external superpositions in the same setup [13].

An alternative route has recently been proposed that relies on entanglement, rather than matter-wave interferometry: one can encode the clocks in photons with different frequencies and use quantum memories [22], or use entangled networks of clocks to accumulate and then interfere different proper time evolutions [23]. The use of quantum networks significantly increases the possible separations of the probe systems and thus also opens up the possibility of testing the coherent dynamics of quantum systems on curved spacetime. However, the test proposed in Ref. [23] does not explicitly probe the effect of the curvature of spacetime, since it only involves the interference of two points in space. Measurements of spacetime curvature (beyond Newtonian gravity) on quantum systems will require distributing the quantum clocks over at least three locations. Such measurements are of particular importance to test quantum theory in this unexplored domain, as curved spacetime may result in modifications to the expected dynamics. However, since the nonlinearity is a higher-order effect in the gravitational potential, more stringent requirements on clock separations and coherence times are necessary to explore this regime.

Here, we propose to use a distributed atomic quantum processor with built-in optical atomic clock functionality to overcome these challenges (see Fig. 1). Specifically, we consider three atomic array quantum processors that are capable of distributing Bell pairs between them via photonic interconnects. We propose a realistic implementation of this system using arrays of ytterbium-171 atoms in optical cavities as network nodes. We demonstrate how this platform can be used to directly measure the curvature of spacetime via an interference fringe of a three-node entangled state, with an approximately kilometer-scale elevation difference between each node. In particular, we discuss how this enables first tests of the linearity and unitarity of quantum theory and tests of the validity of the Born rule in the presence of relativistic spacetime curvature. While arguably challenging, the proposed setup is within reach of state-of-the-art hardware. We also discuss the prospect for employing nonclassical states such as multi-atom Greenberger-Horne-Zeilinger (GHZ) states to effectively amplify the curvature of spacetime.

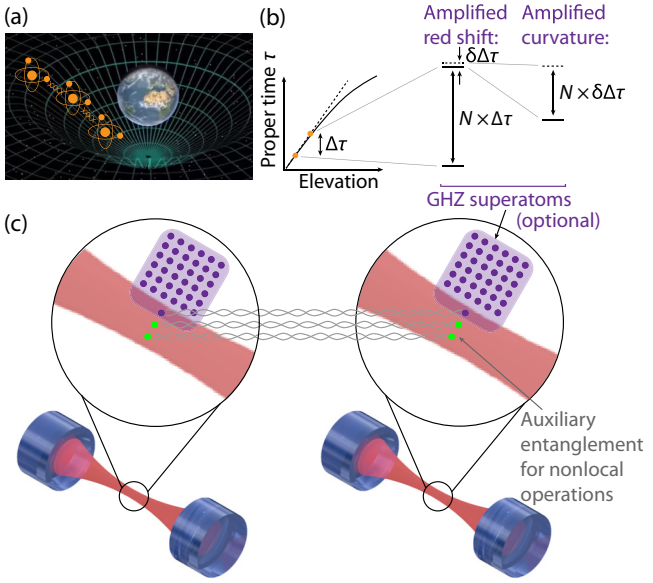

FIG. 1. Probing curved spacetime with entangled clocks. (a) Three atomic clock systems in locations that experience different local gravity share a W state. (b) The Greenberger-Horne-Zeilinger (GHZ) superatoms can boost the bandwidth by amplifying the general-relativistic proper time difference $\Delta\tau$ and nonlinearity $\delta\Delta\tau$ between different elevations, but are otherwise not necessary. (c) The experimental approach. Atomic processor clocks in optical cavities that include the GHZ superatom (purple dots) and auxiliary single-atom Bell pairs for nonlocal operations (green dots).

II. THE ATOMIC SYSTEM AND OVERVIEW OF THE PROTOCOL

Instead of delocalizing an atom to be in a superposition of three distant locations, we use three separated atomic systems and construct a collective quantum state in which we encode one "clock" ("c") and two "not clocks" ("nc") [23]. We encode the "nc" state and the initial part of the "c" state in the nuclear spin-1/2 degree of freedom of the metastable $^3P_0$ state of ytterbium-171 (^{171}Yb) such that the "nc" state $|g\rangle$ is the $m_F = -1/2$ state while the initial "c" state $|a\rangle$ is the $m_F = 1/2$ state [see Fig. 2(a)]. We assume a heralded remote-entanglement protocol that establishes the Bell state

$$|\psi\rangle = \frac{1}{\sqrt{2}}\left(|g,a\rangle + |a,g\rangle\right). \tag{1}$$

Such protocols have been proposed in Refs. [24–27], based on recent demonstrations of atom-photon entanglement and networked atom-atom entanglement of neutral alkali species [28–32], trapped ions [33–36], and solid-state spins [37–41].

We refer to this qubit as "metastable" ("m"), for which $|g\rangle$ and $|a\rangle$. The qubit energy is $E_m/h \approx 100$ kHz at a modest field of approximately 100 G (≈ 1 kHz/G). We denote

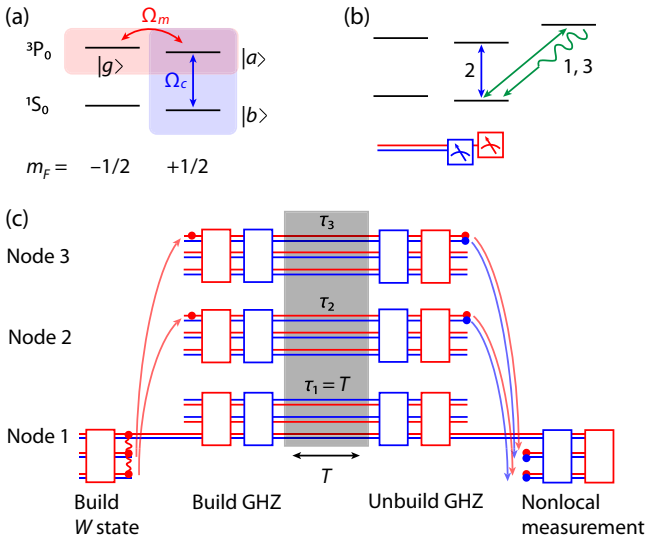

FIG. 2. The atomic system and protocol overview. (a) The relevant level structure of ^{171}Yb. The $\{ga\}$ sector (red) is defined by the nuclear spin qubit in the metastable $^3P_0$ state. The photon-mediated remote-entanglement generation operates in this sector. The clock transition (blue) can be driven both to create coherence on the optical qubit $\{ab\}$ ($\pi/2$ pulse) and also to swap the $\{ga\}$ sector for the $\{gb\}$ sector (π pulse). (b) The three-state qutrit Hilbert space can be measured in two rounds of fluorescence detection in which one or both of the $^1S_0$ ground nuclear spin states is illuminated with probe light. The $^3P_0$ states remain dark and unaffected and a clock π pulse is used between the two rounds. (c) A schematic overview of the circuit. The W-state creation, manipulation, and detection is described in Fig. 3, while the GHZ-state building and unbuilding is described in Fig. 5.

operations on this qubit by pulses with Rabi frequency Ω_m [see Fig. 2(a)] and color them red. Arbitrary fast and high-fidelity qubit manipulations have been demonstrated [42–44] and a coherence time of approximately 7 s has been observed [42]. Additionally, high-fidelity Rydberg-mediated two-qubit controlled-phase (CZ) gates have been demonstrated [43–45]. We assume that $|a\rangle$ is the only state coupled to a Rydberg state. Other two-qubit gates, such as controlled-NOT (CNOT) gates, can be constructed by sandwiching the CZ gate with single-qubit operation on the target qubit, such as with Hadamards in the case of the CNOT gate.

The optical atomic clock qubit is defined by $|a\rangle$, $m_F = 1/2$ in the metastable $^3P_0$ state, and $|b\rangle$, $m_F = 1/2$ in the ground $^1S_0$ state [see Fig. 2(a)]. The qubit energy is $E_c/h \approx 520$ THz. We denote operations on this qubit by pulses with Rabi frequency Ω_c and color them blue. Arbitrary fast and high-fidelity qubit manipulations have been demonstrated on optical qubits [42,46] and a coherence time of approximately 30 s has been observed for state-of-the-art optical clocks [47,48]. Additionally, high-fidelity Rydberg-mediated two-qubit CZ gates have been demonstrated on optical qubits [49,50]. Again, we assume that $|a\rangle$ is the only state coupled to a Rydberg state. Only a modest Zeeman splitting is required to completely decouple the $^1S_0$ $m_F = -1/2$ state from the other three, given the large differential g factor between the metastable and ground nuclear spins [42,51]. Hence, we can choose the sector for which a CNOT gate is applied simply by choosing whether the constituent Hadamard gates operate in the metastable sector (red, via pulses with Ω_m) or the optical-clock sector (blue, via pulses with Ω_c). This versatility is afforded by the more general "omg" architecture [42,52].

Before describing the protocol, we note that our state will generally reside within the $\{gab\}$ qutrit Hilbert space. We must therefore devise a readout protocol that can differentiate these three states, which will require two rounds. In Fig. 2(b), we show this readout operation, in which fluorescence readout is applied to one or both of the nuclear spin $^1S_0$ ground states, leaving the metastable manifold dark and unaffected. By placing a π pulse on the clock transition between the two readout operations [53–55], we can uniquely identify the state of the qutrit (assuming that the atom has not been lost—a possibility that could be detected with a third measurement round).

The protocol is schematically depicted in Fig. 2(c), in which we have three atomic processor nodes that share Bell pairs as an initial resource (see below for further details). First, we construct a three-qubit W state

$$|W\rangle = \frac{1}{\sqrt{3}}\left(|a,g,g\rangle + |g,a,g\rangle + |g,g,a\rangle\right) \qquad (2)$$

in node 1, which resides in the $\{ga\}$ sector. We then teleport two of these qubits to nodes 2 and 3. From here, we could either begin the distributed clock-interrogation protocol or we could amplify the effective qubit energy by N times by spreading the state of each qubit into an N-atom GHZ state in each node. In either case, our atoms now reside in the full $\{gab\}$ qutrit space. We probe the differential proper time for a duration T (as measured in node 1) and then we prepare for measurement. First, we unbuild the GHZ state if we used it and then we teleport the qutrits in nodes 2 and 3 back to node 1. Finally, we perform a nonlocal measurement that is blind to the identity of our three atoms, yet results in a periodic loss and revival of the visibility of interferometric "self-interference" between all three clocks as a signature of the interplay of quantum dynamics and general relativistic proper time evolution.

We assume that the "master-clock laser" is in node 1 and is referenced to a separate atomic clock to ensure long-term phase stability with respect to atoms. The "master clock" also defines the "wall time" T for each node. The stability of this laser is transferred to nodes 2 and 3 via standard phase-stabilized fiber-link techniques [56–58], where it is used to "lock" the local oscillators in nodes 2 and 3, ensuring a common frequency reference in all nodes. This approach is ubiquitous in classical clock networks [57–60].

III. SIGNATURE OF QUANTUM INTERFERENCE IN THE PRESENCE OF SPACETIME CURVATURE

We now discuss how to create, distribute, and detect W states in order to obtain a quantum interference signal of proper times that contains signatures of curved spacetime. We begin by building the distributed W state locally in node 1 and then teleport two of its constituent qubits to nodes 2 and 3. This circuit is shown in Fig. 3(a), where the standard qubit-teleportation protocol based on auxiliary entanglement is shown in Fig. 3(b). The W state resides in the $\{ga\}$ sector. After building the nonlocal W state (neglecting the GHZ state for now), we start the nonlocal clock by applying a $\pi/2$ rotation in the $\{ab\}$ subspace similar to the protocol of Ref. [23]. The resulting state after a certain free evolution time is

$$\begin{aligned}|W_T\rangle = \frac{1}{\sqrt{6}}\Big(&\left(|a\rangle + e^{-i\theta_1}|b\rangle\right)|g\rangle|g\rangle \\ &+ e^{-i\phi_1}|g\rangle\left(|a\rangle + e^{-i\theta_2}|b\rangle\right)|g\rangle \\ &+ e^{-i\phi_2}|g\rangle|g\rangle(|a\rangle + e^{-i\theta_3}|b\rangle)\Big),\end{aligned} \tag{3}$$

where $\theta_j = (E_b - E_a)\tau_j/\hbar = \Delta E\tau_j/\hbar$, $\phi_j = (E_g - E_a)(\tau_1 - \tau_{j+1})/\hbar$, and τ_j is the proper time at the jth node. The states $|c(\tau_i)\rangle \equiv \frac{1}{\sqrt{2}}(|a\rangle + e^{-i\theta_1}|b\rangle)$ are the local clock states that record the proper time τ_i, which depends on the position in the gravitational field. We must now perform a nonlocal measurement of our W state. We first teleport our qutrits back to node 1 such that all subsequent operations are local [see Fig. 3(c)]. Naturally, teleporting a qutrit is more advanced than teleporting a qubit and two auxiliary Bell pairs are required for each qutrit. As shown in Fig. 3(d), the qutrit teleportation can be performed in two rounds. A phase correction on the teleported qutrit state conditional on the teleportation-measurement outcomes may be required. Then, the final step involves a quantum Fourier transform of our initial qutrit followed by measurement.

Once all the qutrits are in node 1, we use an ancilla qubit to measure the state of the clock qubit without revealing its location. First, we perform a Hadamard gate in the $\{ab\}$ subspace on each system. After this, we perform a series of CNOT gates in the $\{ab\}$ sector, with each qutrit in the W state serving as a control and the ancilla serving as the target such that a subsequent measurement of the ancilla qubit will project the state into either the $\{ga\}$ or $\{gb\}$ subspace.

We then apply a global X pulse in the $\{ab\}$ sector conditional on the ancilla-measurement outcome to ensure that the postmeasurement state is entirely in the $\{ga\}$ subspace and will be of the form

$$\begin{aligned}|\psi_\pm\rangle = \frac{1}{6}\Big(&\left(1 \pm e^{-i\theta_1}\right)|a,g,g\rangle + e^{-i\phi_1}\left(1 \pm e^{-i\theta_2}\right)|g,a,g\rangle \\ &+ e^{-i\phi_2}\left(1 \pm e^{-i\theta_3}\right)|g,g,a\rangle\Big),\end{aligned} \tag{4}$$

with $|\psi_+\rangle$ ($|\psi_-\rangle$) corresponding to measuring the auxiliary atom in state $|a\rangle$ ($|b\rangle$). The norm $|\langle\psi_+|\psi_+\rangle|^2$ ($|\langle\psi_-|\psi_-\rangle|^2$) corresponds to the probability of measuring $|a\rangle$ ($|b\rangle$). To interfere the three clock locations, we subsequently perform a measurement in the Fourier basis $\{|x\rangle\}$, where

$$|x\rangle = \frac{1}{\sqrt{3}}\left(|a,g,g\rangle + e^{iw_x}|g,a,g\rangle + e^{2iw_x}|g,g,a\rangle\right), \tag{5}$$

with $w_x = 2\pi x/3$ and $x \in \{0,1,2\}$. Defining the projectors, $\Pi_x = |x\rangle\langle x|$, we see that

$$\begin{aligned}\langle\Pi_x\rangle &= \langle\psi_+|\Pi_x|\psi_+\rangle + \langle\psi_-|\Pi_x|\psi_-\rangle \\ &= \frac{1}{9}\big(3 + \cos(w_x - \phi_2 + \phi_1) \\ &\quad + \cos(\theta_1 - \theta_2 - w_x - \phi_1) \\ &\quad + \cos(2w_x - \phi_2) + \cos(\theta_1 - \theta_3 - 2w_x - \phi_2) \\ &\quad + \cos(w_x - \phi_1) + \cos(\theta_3 - \theta_2 + w_x + \phi_2 - \phi_1)\big) \\ &= \frac{1}{3} + \frac{2}{9}\big(|\langle c(\tau_1)|c(\tau_2)\rangle|\cos(\lambda_{12} - w_x - \phi_1) \\ &\quad + |\langle c(\tau_1)|c(\tau_3)\rangle|\cos(\lambda_{13} - 2w_x - \phi_2) \\ &\quad + |\langle c(\tau_2)|c(\tau_3)\rangle|\cos(\lambda_{23} - w_x - \phi_2 + \phi_1)\big),\end{aligned} \tag{6}$$

where we have defined $|c(\tau_i)\rangle = \frac{1}{\sqrt{2}}(|a\rangle + e^{-i\Delta E\tau_i/\hbar}|b\rangle)$, and $\langle c(\tau_i)|c(\tau_j)\rangle = |\langle c(\tau_i)|c(\tau_j)\rangle|e^{-i\lambda_{ij}}$. From Eq. (6), we see that the measured projectors exhibit oscillating terms due to the gravitational time dilation between all pairwise combinations of the three clock locations.

The observable captures interference of the three proper time evolutions at their respective locations, which provides a genuine test of quantum mechanics in curved spacetime. As an example, we consider a scenario in which the three locations are placed at distances $d_j = jd$ ($j \in 0,1,2$) from Earth's surface. For ^{171}Yb, we have that $E_g \approx E_a$ while $(E_a - E_b)/h = -\Delta E/\hbar \approx 520\,\mathrm{THz}$. The measured signal $\langle\Pi_x\rangle$ for any choice of x would exhibit oscillations with the three frequencies

$$\omega_{12} = \frac{\partial}{\partial t}(\theta_1 - \theta_2) = \frac{\Delta EGM}{\hbar c^2}\left(\frac{1}{R} - \frac{1}{R+d}\right), \tag{7}$$

$$\omega_{23} = \frac{\partial}{\partial t}(\theta_2 - \theta_3) = \frac{\Delta EGM}{\hbar c^2}\left(\frac{1}{R+d} - \frac{1}{R+2d}\right), \tag{8}$$

$$\omega_{13} = \frac{\partial}{\partial t}(\theta_1 - \theta_3) = \frac{\Delta EGM}{\hbar c^2}\left(\frac{1}{R} - \frac{1}{R+2d}\right). \tag{9}$$

To first order, we see that $\omega_{12} \approx \omega_{23}$, but the effect of curvature is visible in the higher-order terms since

$$\Delta\omega = \omega_{12} - \omega_{23} \approx 2\frac{\Delta EGM}{\hbar c^2}\frac{d^2}{R^3}, \tag{10}$$

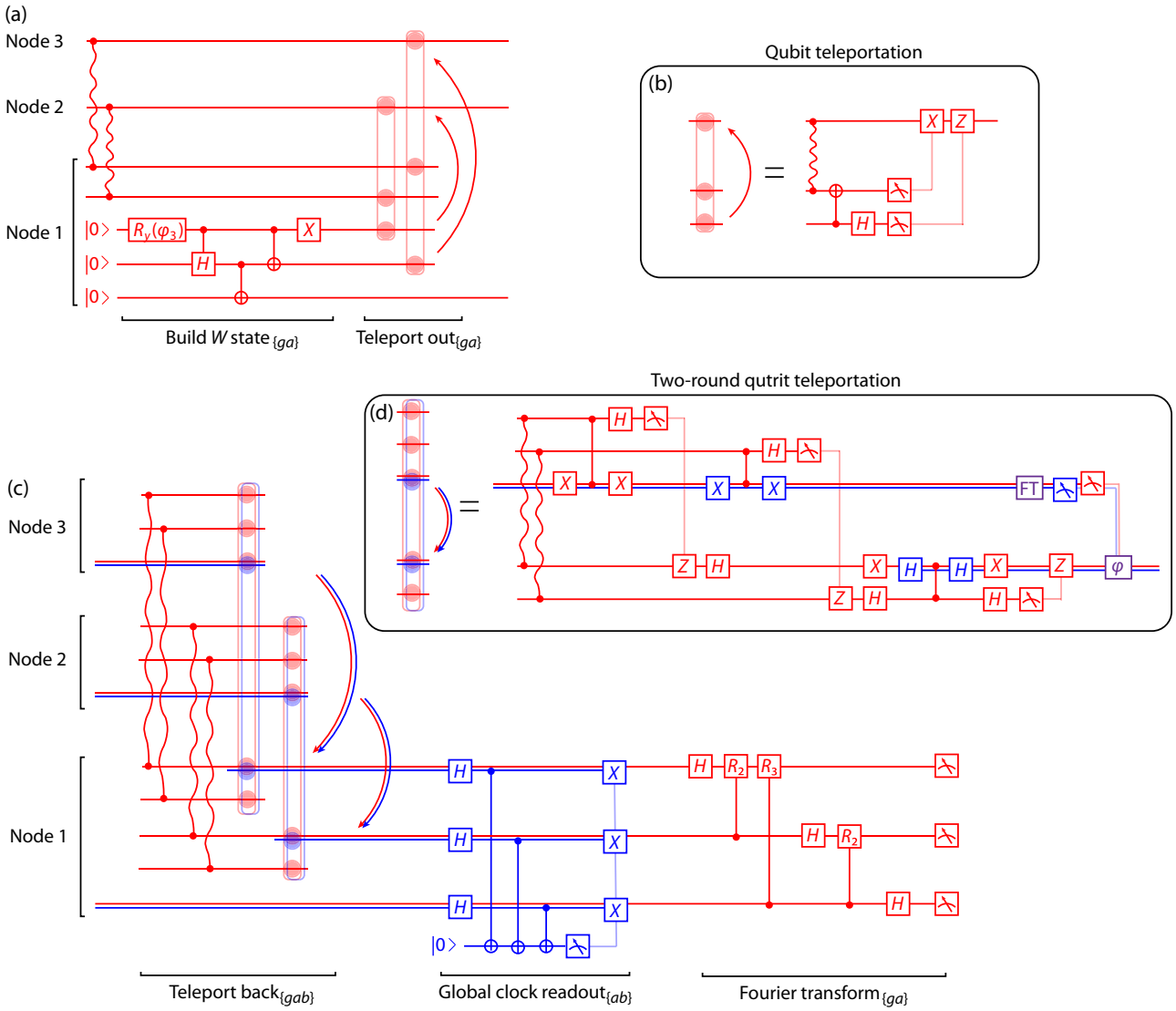

FIG. 3. Creating, distributing, and detecting W states. (a) To initialize a distributed W state, we begin by distributing a Bell pair between nodes 1 and 2 and a Bell pair between nodes 1 and 3. Then, we produce a three-atom W state in node 1 in the $\{ga\}$ sector, where $\phi_3 = 2\arccos(1/\sqrt{3})$. We teleport two qubits in the W state, one each to nodes 2 and 3 using a standard qubit-teleportation protocol shown in (b) and based on auxiliary entanglement. Then, a GHZ state may be built and unbuilt within each node, following the protocol in Fig. 5, sandwiched around an interrogation of GR through proper time measurements as above. (c) This leaves us in a distributed W state in the $\{gab\}$ qutrit space. We begin by teleporting the qutrits in nodes 2 and 3 back to node 1 using two Bell pairs each of auxiliary entanglement. The two-round qutrit-teleportation protocol is shown in (d). Once the qutrit W state has been returned to node 1, an ancilla-based nonlocal probe of whether the clock qubit is in $|a\rangle$ or $|b\rangle$ (called a "global clock readout") is performed, followed by a conditional global X operation on the $\{ab\}$ sector. Then, a Fourier transform is applied for nonlocal readout of the $\{ga\}$ sector.

to leading order. The resulting post-Newtonian frequency shift thus shows simultaneous effects of both curved spacetime and quantum interference. To resolve this frequency, we need to let the system evolve for a total "wall time" of

$$T \approx \frac{1}{\Delta\omega} = \frac{\hbar R^3 c^2}{2d^2 \Delta E G M}. \tag{11}$$

In Fig. 4, we plot $\langle \Pi_0 \rangle$ from three single-atom clocks for $d = 1$ km. It can be seen that for a single-atom coherence time of $T_2 = 50$ s, it is possible to resolve $\Delta\omega \sim 0.02$ Hz for a total evolution time of $T = 500$ s. Although obtaining such coherence times is challenging, it is within reach of current hardware [47,48]. Moreover, "spectator" ancilla qubits could be employed to track and compensate global magnetic field noise [61], which is the leading source of decoherence for nuclear Zeeman states.

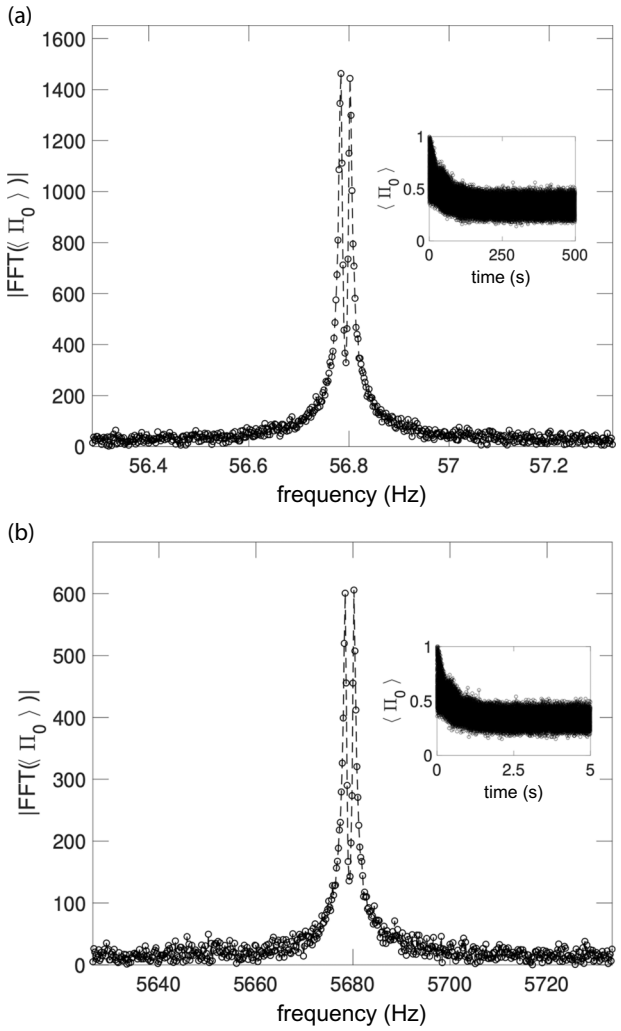

FIG. 4. (a) The fast Fourier transform of our nonlocal clock observable of interest in Eq. (6), $\langle \Pi_0 \rangle$, assuming three atoms positioned at Earth's surface, 1 km, and 2 km above the surface, respectively. The signal is sampled at a rate of 0.5 kHz for a total evolution time of $T = 500$ s. Each data point is calculated as the mean of 100 samples and we have assumed that the atoms are subject to dephasing noise corresponding to $T_2 = 50$ s. The line splitting arises due to spacetime curvature. The inset shows the sampled signal as a function of time. (b) The same plot but for three GHZ superatoms with $N = 100$. The sampling rate is 10 kHz and we have assumed an effective GHZ dephasing time of 0.5 s.

IV. ENTANGLEMENT-ENHANCED SENSING USING GHZ SUPERATOMS

One challenge with the assumed $T_2 = 50$ s and $T = 500$ s for this measurement is the presence of technical noise sources that can have a nonlinear dependence on the interrogation time. These can include thermal effects in stabilization electronics for optical potentials and magnetic fields and even heating of the atom in an optical trap due to intensity noise. Moreover, we propose to perform this experiment in a terrestrial network, which will require one node to be at the top of a tall building. Therefore, we must be careful to obviate the effects of natural low-frequency oscillations. Because of these effects and others, the "wall-clock" time for this experiment is an important consideration and methods to boost the measurement bandwidth are worth considering.

It is possible to boost $\Delta\omega$ without increasing the separation between the atomic nodes. We can employ N-atom GHZ states in each system to effectively create a "superatom" with an N-times-larger clock-transition energy. The protocol for creating and performing the Ramsey interrogation with the GHZ state is shown in Fig. 5(a). We again start with the W state

$$|W\rangle = \frac{1}{\sqrt{3}}\left(|a,g,g\rangle + |g,a,g\rangle + |g,g,a\rangle\right) \tag{12}$$

and then we build a GHZ state in each module through the use of cascaded CNOT gates with the other $N-1$ qubits that were initially in $|g\rangle$. This creates the state

$$|\psi\rangle = \frac{1}{\sqrt{6}}\left(|a\rangle^{\otimes N}|g\rangle^{\otimes N}|g\rangle^{\otimes N} + |g\rangle^{\otimes N}|a\rangle^{\otimes N}|g\rangle^{\otimes N} + |g\rangle^{\otimes N}|g\rangle^{\otimes N}|a\rangle^{\otimes N}\right). \tag{13}$$

The local GHZ states resides in the $\{ga\}$ sector and we must similarly build GHZ states in the $\{ab\}$ sector to start the nonlocal clock. We apply a $\pi/2$ pulse on the clock transition of the "science" atoms and then perform the cascaded CNOT gates, now in the $\{ab\}$ sector [blue in Fig. 5(a)].

We are now in the state

$$|\psi^{\mathrm{GHZ}}\rangle = \frac{1}{\sqrt{6}}\left(\left(|a\rangle^{\otimes N} + |b\rangle^{\otimes N}\right)|g\rangle^{\otimes N}|g\rangle^{\otimes N} + |g\rangle^{\otimes N}\left(|a\rangle^{\otimes N} + |b\rangle^{\otimes N}\right)|g\rangle^{\otimes N} + |g\rangle^{\otimes N}|g\rangle^{\otimes N}\left(|a\rangle^{\otimes N} + |b\rangle^{\otimes N}\right)\right). \tag{14}$$

After the evolution under the presence of differential proper time, we are in the state

$$|\psi_T^{\mathrm{GHZ}}\rangle = \frac{1}{\sqrt{6}}\left(\left(|a\rangle^{\otimes N} + e^{-iN\theta_1}|b\rangle^{\otimes N}\right)|g\rangle^{\otimes N}|g\rangle^{\otimes N} + e^{-iN\phi_1}|g\rangle^{\otimes N}\left(|a\rangle^{\otimes N} + e^{-iN\theta_2}|b\rangle^{\otimes N}\right)|g\rangle^{\otimes N} + e^{-iN\phi_2}|g\rangle^{\otimes N}|g\rangle^{\otimes N}\left(|a\rangle^{\otimes N} + e^{-iN\theta_3}|b\rangle^{\otimes N}\right)\right). \tag{15}$$

To interfere the clock state of the different locations, the measurement protocol must be compatible with the nonlocal measurement circuits shown in Figs. 2 and 3. As such, we want to remove the extra $N-1$ qubits used

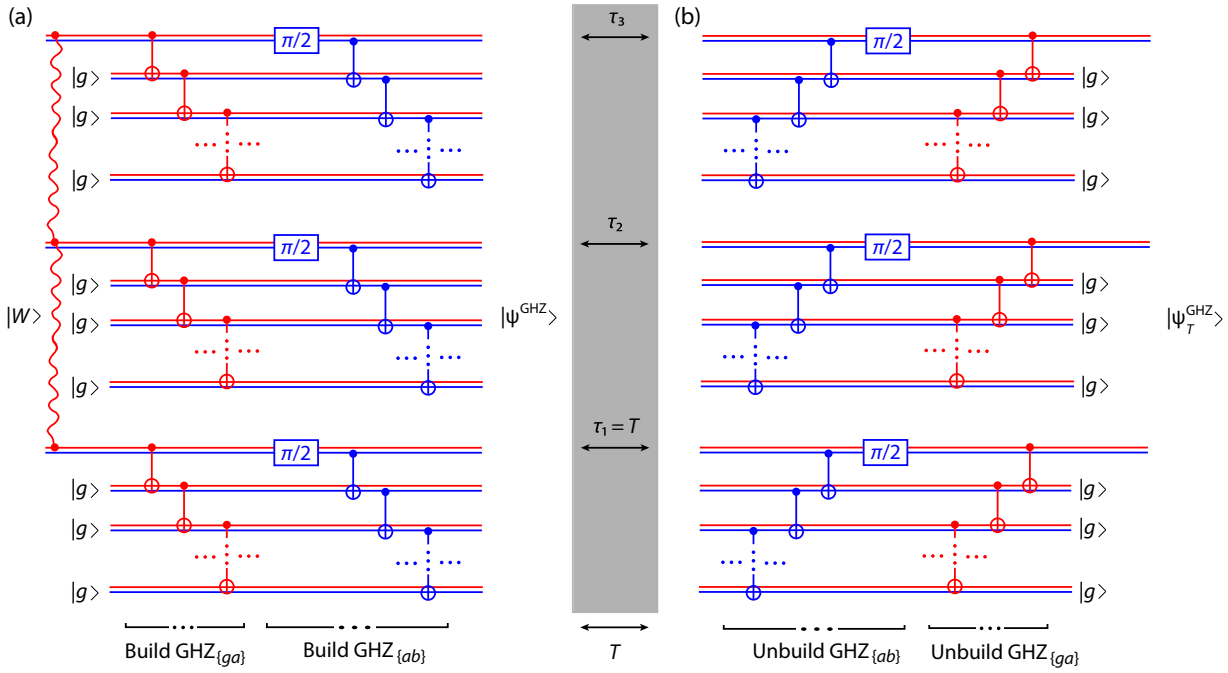

FIG. 5. Building and unbuilding distributed GHZ superatoms. (a) We begin with the distributed W state $|W\rangle$ from Fig. 3 as well as $N-1$ additional qubits initialized in $|g\rangle$. We then build a GHZ state in the $\{ga\}$ sector in each module with cascaded CNOT gates. The resulting state is now a version of $|W\rangle$ in which every single-atom state is raised to the $\otimes N$. Then, we apply a $\pi/2$ pulse to the clock transition on the "science" qubits and use them to grow a GHZ state in the $\{ab\}$ sector using cascaded CNOT gates that operate in that sector (blue; $|a\rangle \equiv |1\rangle$ and $|b\rangle \equiv |0\rangle$). Then, the clock Ramsey interferometer now works in the same way as the single-atom case, except that the effective phase accrual due to the difference in proper time is N times larger. This can be equivalently viewed as a single superatom with an N-times-larger clock-transition energy. Note that this distributed GHZ state spans the $\{gab\}$ qutrit space, like the single-atom case. (b) To measure this state, we must unbuild the GHZ states such that we can perform the nonlocal measurement. We unbuild in both the $\{ab\}$ and $\{ga\}$ sectors with cascaded CNOT gates, essentially running time backward compared to the build operations. The additional $N-1$ qubits in each module return to $|g\rangle$ and the "science" W state is in a phase-multiplied version of the state $|W_T\rangle$. We can now apply the protocol from Fig. 3 for nonlocal measurement.

in the GHZ superatom in each system. We thus unbuild the GHZ state, as shown in Fig. 5(b). The protocol again uses cascaded CNOT gates in reverse order, essentially to "undo" the entanglement from the cascaded CNOT gates in the building process. We begin in the $\{ab\}$ sector by applying the cascaded CNOT gates and the $\pi/2$ pulses on the clock transition of the "science" atoms. We then unbuild the GHZ state in the $\{ga\}$ sector. This leaves us in the state shown in Eq. (3), except that all phases have been multiplied by a factor of N. The final nonlocal measurement can now be performed as previously described for the simple W state.

Using GHZ superatoms, we effectively increase the interrogation bandwidth of the tests by a factor of N, allowing for a much shorter interrogation time. In Fig. 4(b), we plot $\langle \Pi_0 \rangle$ from three GHZ superatoms at separations of $d = 1$ km. Each superatom consists of $N = 100$ atoms and we have assumed an effective dephasing time of the GHZ-state superatoms of 0.5 s (N times faster). It is possible to resolve $\Delta\omega \sim 2$ Hz for a total evolution time of 5 s.

V. TESTING QUANTUM THEORY ON CURVED SPACETIME

The central science goal of this proposal is to observe how quantum dynamics and general relativistic curved spacetime intertwine, in a single observable. If one of those theories are modified in this regime, the outcome would be different than predicted here. The key observable is given in Eq. (6). It shows the interference of the clock state overlaps $\langle c(\tau_x)|c(\tau_y)\rangle$, which are different from unity due to the different general relativistic proper time evolutions $U(\tau_x)$ at the locations of the clocks. The observable involves not just these proper time evolutions as in regular clock measurements but also their quantum interference. Spacetime curvature manifests itself in the scaling of the proper times: they are no longer changing linearly with height h as $\Delta\tau = ght/c^2$, which would also be the case in special relativistic acceleration. The observable thus cannot be mapped from gravity to special relativity according to the equivalence principle, as curved spacetime induces a nonlinear spatial scaling between the different proper times. This manifests

itself in the line splitting in frequency space of the observables $\langle \Pi_x \rangle$, as in Fig. 4. The test also clearly goes beyond any Newtonian curvature effect, as the observable is due to the general relativistic proper time. This is in contrast to already performed superposition experiments with atomic fountains that are sensitive to spacetime curvature in the Newtonian limit [62].

In what way could the outcomes differ from expected physics? When gravity and quantum theory intertwine, deviations from regular quantum physics might emerge [63–66] and no empirical evidence of the validity of quantum theory in this regime exists so far. Our protocol enables several critical tests of this domain. First, as outlined in Ref. [23], such an experiment with entangled clocks can be used to directly test the unitarity and linearity of quantum theory on curved spacetime. To this end, one can compare two different experimental protocols: one using entangled clocks as proposed above and another one with initially separable clocks and the same nonlocal measurement operators Π_x. The latter should also produce the exact same *conditional* outcome as in Eq. (6) but with finite success probability. This is because in normal linear and unitary quantum evolution, the nonlocal contribution is one of many amplitudes that contribute to the same outcome, even for initial product states. It can be easily seen when writing the state in terms of Bell states, which constitute a basis. Explicitly, the protocol for the conditional experiment would be the following: one first prepares the three clocks in the product state $|\Psi(0)\rangle = (\frac{1}{\sqrt{3}}(|g\rangle + \sqrt{2}|c(0)\rangle))^{\otimes 3}$, where $|c(0)\rangle = \frac{1}{\sqrt{2}}(|a\rangle + |b\rangle)$. The states evolve to $|\Psi\rangle = \frac{1}{\sqrt{27}}\Pi_{i=1}^{\otimes 3}(e^{-iE_g\tau_i}|g\rangle + \sqrt{2}e^{-iE_b\tau_i}|c(\tau_i)\rangle)_i$. This state, while being a product state, has also the amplitude $\sqrt{\frac{2}{9}}e^{-i\varphi}|W_T\rangle$ from Eq. (3), on which we conditionally project yielding the same outcome as in Eq. (6). Thus the comparison of outcomes between the initially entangled and product states would provide a direct test of unitarity and linearity of quantum theory even when the dynamics must include general relativistic corrections. The only other performed test of unitarity in the presence of spacetime curvature, to our knowledge, has focused on the propagation of photons in Earth's gravitational field to test for anomalous decoherence [67]. Our proposed test with time dilation of entangled clocks would broaden the scope to test the validity of quantum theory for genuine general relativistic observables.

Second, our protocol explores the quantum dynamics with gravitational corrections both in the general relativistic limit and beyond the homogeneous limit. This opens up new opportunities to test gravity in quantum theory, as one can see from a semiclassical phase-space picture: as long as the potentials are at most quadratic in position, the dynamics, if represented by a Wigner quasiprobability distribution, are indistinguishable from a classical Liouville equation. Thus no quantum contributions arise from the dynamics in this limit [68]. However, this mapping breaks down when the dynamics become non-Gaussian. Pushing into this limit enables tests of how curved spacetime may affect the quantum dynamics in anomalous ways [69]. Our protocol operates in this limit and the proper time observables enable the exploration of such possibly anomalous dynamics in the post-Newtonian regime. To probe genuine quantum dynamics in the Wigner evolution amounts to observing time-dilation differences due to nonlinear potential differences beyond the second order, when Eq. (10) gets the additional contribution $\Delta\omega_3 \approx 5((\Delta EGM)/\hbar c^2)(d^3/R^4)$.

Third, our test also provides a novel exploration of one of the most fundamental principles of quantum theory: the Born rule. One of its core consequences is interference of amplitudes, where the probability of superposed configurations P_{12} leads to interference I_{12} in addition to the individual probabilities, $P_{12} = P_1 + P_2 + I_{12}$. Higher-order interference, however, does not arise [70], as the Born rule results only in pairwise interference terms. Our observable in Eq. (6) is constructed from three-path interference of the three clocks, as indicative by the projection measurement in the Fourier basis, given in Eq. (5). One can combine such measurements with observables constructed only with two clocks interfering, or even just individual clocks. One can construct the second-order interference quantity

$$I_{123} = P_{123} - P_{12} - P_{13} - P_{23} + P_1 + P_2 + P_3, \quad (16)$$

where the P_{ijk} correspond to the probabilities of obtaining the observable with the clocks in the respective positions. In regular quantum theory, this quantity exactly vanishes ($I_{123} = 0$) due to the Born rule. However, higher-order interferences that go beyond the Born rule would show in a nonzero value. This has been used to experimentally test the Born rule [71,72]. It has also been suggested that quantum gravity might result in modifications to the Born rule [73–76], with early explorations by Sorkin [70]. Our protocol here can easily implement the measurement in Eq. (16) in analogy to Ref. [72]. We measure directly the three-part interference P_{ijk}, which is what the outcome (6) yields. One can now extend the protocol to also measure only two-clock interferences, and even single clock measurements as required by Eq. (16). To compare them, one has to make sure that the amplitudes remain unchanged from $1/\sqrt{3}$. This simply requires an additional ancillary state as in Ref. [72], which again is straightforward to implement in our protocol. Thus the setup that we propose can easily be used to probe the Born rule and can therefore provide the first empirical test of one of the most fundamental principles of quantum theory under the influence of general relativity.

VI. CONCLUDING DISCUSSION

Using quantum networking techniques, we have proposed a protocol to probe general relativistic time dilation due to the curvature of Earth's gravitational potential via three entangled atomic systems with approximately kilometer-scale separation. Our proposal combines many state-of-the-art techniques in atomic quantum science, ranging from quantum networking [30] to quantum algorithms [77,78] to quantum metrology [46,50]. Further, we utilize qutrit code spaces composed of nuclear and optical-clock degrees of freedom, with inspiration from recent work on qudit [79] and multiqubit encodings [55] in atomic systems. We have mostly focused on neutral ytterbium-171 atoms but our protocols could equally be applied to trapped-ion systems. Recently, remote entanglement between two ions with a fidelity of 0.97 has been demonstrated by using a time-bin encoding scheme [36] and entanglement between the nuclear spin and a telecom-band photon in neutral ytterbium-171 atoms has recently been demonstrated with a fidelity of 0.95 [32]. Given the demonstrated coherence times of nuclear spin qubits (approximately 7 s) [42] and the demonstrated half-minute-scale atom-atom coherence of optical-clock qubits [47,48], as well as the demonstrated Rydberg-mediated gate fidelities of approximately 0.995 across several different qubit encodings [44–46,80,81], we anticipate that it may be feasible to realize approximately 100-atom GHZ states in each node with fidelity above approximately 0.5.

The proposed setup enables unique tests of the interplay of quantum theory and general relativity—where no such tests have yet been performed. We have shown that it can test whether some of the most fundamental tenets of quantum theory survive in the presence of spacetime curvature, focusing on the interference of general relativistic proper time evolutions. Our proposed tests of the unitarity, linearity, and the probabilistic Born rule of quantum theory enable the first exploration of the interplay of the foundations of quantum theory and general relativity in a realistic experiment with quantum networks, opening the door for unique new ground-based and space-based tests of quantum physics and general relativity.

ACKNOWLEDGMENTS

J.P.C. acknowledges funding from the National Science Foundation (NSF) Quantum Leap Challenge Institute (QLCI) for Hybrid Quantum Architectures and Networks (NSF Award No. 2016136); the NSF Division of Physics (PHY) (NSF Awards No. 2112663 and No. 2339487); the NSF Quantum Interconnects Challenge for Transformational Advances in Quantum Systems (QuIC-TAQS) (NSF Award no. 2137642); the Office for Nuclear Regulation (ONR) Young Investigator Program (ONR Award No. N00014-22-1-2311); the Air Force Office of Scientific Research (AFOSR) Young Investigator Program (AFOSR Award No. FA9550-23-1-0059); and the U.S. Department of Energy Office of Science, National Quantum Information Science Research Centers. I.P. acknowledges support by the NSF under Award No. 2239498, the National Aeronautics and Space Administration (NASA) under Award No. 80NSSC25K7051 and the Sloan Foundation under Award No. G-2023-21102. J.B. acknowledges support from The AWS Quantum Discovery Fund at the Harvard Quantum Initiative.

DATA AVAILABILITY

The data supporting this study's findings are available within the article.

[1] D. Oriti, *Approaches to Quantum Gravity: Toward a New Understanding of Space, Time and Matter* (Cambridge University Press, 2009).

[2] S. A. Fulling, *Aspects of Quantum Field Theory in Curved Spacetime* (Cambridge University Press, Cambridge, UK, 1989), Vol. 17.

[3] D. Carney, P. C. Stamp, and J. M. Taylor, Tabletop experiments for quantum gravity: A user's manual, Class. Quantum Grav. **36**, 034001 (2019).

[4] S. Bose, I. Fuentes, A. A. Geraci, S. M. Khan, S. Qvarfort, M. Rademacher, M. Rashid, M. Toroš, H. Ulbricht, and C. C. Wanjura, Massive quantum systems as interfaces of quantum mechanics and gravity, Rev. Mod. Phys. **97**, 015003 (2025).

[5] C. Marletto and V. Vedral, Quantum-information methods for quantum gravity laboratory-based tests, Rev. Mod. Phys. **97**, 015006 (2025).

[6] L. Lami, J. S. Pedernales, and M. B. Plenio, Testing the quantumness of gravity without entanglement, Phys. Rev. X **14**, 021022 (2024).

[7] G. Tobar, S. K. Manikandan, T. Beitel, and I. Pikovski, Detecting single gravitons with quantum sensing, Nat. Commun. **15**, 7229 (2024).

[8] R. Colella, A. W. Overhauser, and S. A. Werner, Observation of gravitationally induced quantum interference, Phys. Rev. Lett. **34**, 1472 (1975).

[9] C. Overstreet, P. Asenbaum, J. Curti, M. Kim, and M. A. Kasevich, Observation of a gravitational Aharonov-Bohm effect, Science **375**, 226 (2022).

[10] V. V. Nesvizhevsky, H. G. Börner, A. K. Petukhov, H. Abele, S. Baeßler, F. J. Rueß, T. Stöferle, A. Westphal, A. M. Gagarski, G. A. Petrov, *et al.*, Quantum states of neutrons in the Earth's gravitational field, Nature **415**, 297 (2002).

[11] T. Jenke, D. Stadler, H. Abele, and P. Geltenbort, Q-BOUNCE—experiments with quantum bouncing ultracold neutrons, Nucl. Instrum. Methods Phys. Res., Sect. A **611**, 318 (2009).

[12] S. Dimopoulos, P. W. Graham, J. M. Hogan, and M. A. Kasevich, General relativistic effects in atom interferometry, Phys. Rev. D: Part. Fields Gravitat. Cosmol. **78**, 042003 (2008).
[13] M. Zych, F. Costa, I. Pikovski, and Č. Brukner, Quantum interferometric visibility as a witness of general relativistic proper time, Nat. Commun. **2**, 505 EP (2011).
[14] S. Sinha and J. Samuel, Atom interferometry and the gravitational redshift, Class. Quantum Grav. **28**, 145018 (2011).
[15] I. Pikovski, M. Zych, F. Costa, and Č. Brukner, Universal decoherence due to gravitational time dilation, Nat. Phys. **11**, 668 (2015).
[16] M. Zych, I. Pikovski, F. Costa, and Č. Brukner, in *Journal of Physics: Conference Series* (IOP Publishing, Potsdam, Germany, 2016), Vol. 723, p. 012044.
[17] P. J. Orlando, F. A. Pollock, and K. Modi, in *Lectures on General Quantum Correlations and Their Applications*, edited by F. Fanchini, D. Soares Pinto, and G. Adesso (Springer, Cham, 2017), p. 421.
[18] Z. Zhou, Y. Margalit, D. Rohrlich, Y. Japha, and R. Folman, Quantum complementarity of clocks in the context of general relativity, Class. Quantum Grav. **35**, 185003 (2018).
[19] S. Loriani, A. Friedrich, C. Ufrecht, F. Di Pumpo, S. Kleinert, S. Abend, N. Gaaloul, C. Meiners, C. Schubert, D. Tell, *et al.*, Interference of clocks: A quantum twin paradox, Sci. Adv. **5**, eaax8966 (2019).
[20] A. Roura, Gravitational redshift in quantum-clock interferometry, Phys. Rev. X **10**, 021014 (2020).
[21] Y. Margalit, Z. Zhou, S. Machluf, D. Rohrlich, Y. Japha, and R. Folman, A self-interfering clock as a "which path" witness, Science **349**, 1205 (2015).
[22] R. Barzel, M. Gündoğan, M. Krutzik, D. Rätzel, and C. Lämmerzahl, Entanglement dynamics of photon pairs and quantum memories in the gravitational field of the earth, Quantum **8**, 1273 (2024).
[23] J. Borregaard and I. Pikovski, Testing quantum theory on curved spacetime with quantum networks, Phys. Rev. Res. **7**, 023192 (2015).
[24] J. P. Covey, A. Sipahigil, S. Szoke, N. Sinclair, M. Endres, and O. Painter, Telecom-band quantum optics with ytterbium atoms and silicon nanophotonics, Phys. Rev. Appl. **11**, 034044 (2019).
[25] W. Huie, S. G. Menon, H. Bernien, and J. P. Covey, Multiplexed telecommunication-band quantum networking with atom arrays in optical cavities, Phys. Rev. Res. **3**, 043154 (2021).
[26] Y. Li and J. D. Thompson, High-rate and high-fidelity modular interconnects between neutral atom quantum processors, PRX Quantum **5**, 020363 (2024).
[27] S. Sunami, S. Tamiya, R. Inoue, H. Yamasaki, and A. Goban, Scalable networking of neutral-atom qubits: Nanofiber-based approach for multiprocessor fault-tolerant quantum computers, PRX Quantum **6**, 010101 (2025).
[28] J. Hofmann, M. Krug, N. Ortegel, L. Gérard, M. Weber, W. Rosenfeld, and H. Weinfurter, Heralded entanglement between widely separated atoms, Science **337**, 72 (2012).
[29] S. Daiss, S. Langenfeld, S. Welte, E. Distante, P. Thomas, L. Hartung, O. Morin, and G. Rempe, A quantum-logic gate between distant quantum-network modules, Science **371**, 614 (2021).
[30] J. P. Covey, H. Weinfurter, and H. Bernien, Quantum networks with neutral atom processing nodes, npj Quantum Inf. **9**, 90 (2023).
[31] L. Hartung, M. Seubert, S. Welte, E. Distante, and G. Rempe, A quantum-network register assembled with optical tweezers in an optical cavity, Science **385**, 179 (2024).
[32] L. Li, S. Hu, Z. Jia, W. Huie, W. K. C. Sun, Aakash, M. Dong, T. Hiri-O-Tuppa, and J. P. Covey, Parallelized telecom quantum networking with a ytterbium-171 atom array, arXiv:2502.17406.
[33] S. Olmschenk, D. N. Matsukevich, P. Maunz, D. Hayes, L.-M. Duan, and C. Monroe, Quantum teleportation between distant matter qubits, Science **323**, 486 (2009).
[34] L. J. Stephenson, D. P. Nadlinger, B. C. Nichol, S. An, P. Drmota, T. G. Ballance, K. Thirumalai, J. F. Goodwin, D. M. Lucas, C. J. Ballance, High-rate, high-fidelity entanglement of qubits across an elementary quantum network, Phys. Rev. Lett. **124**, 110501 (2020).
[35] B. C. Nichol, R. Srinivas, D. P. Nadlinger, P. Drmota, D. Main, G. Araneda, C. J. Ballance, and D. M. Lucas, An elementary quantum network of entangled optical atomic clocks, Nature **609**, 689 (2022).
[36] S. Saha, M. Shalaev, J. O'Reilly, I. Goetting, G. Toh, A. Kalakuntla, Y. Yu, and C. Monroe, High-fidelity remote entanglement of trapped atoms mediated by time-bin photons, arXiv:2406.01761.
[37] H. Bernien, B. Hensen, W. Pfaff, G. Koolstra, M. S. Blok, L. Robledo, T. H. Taminiau, M. Markham, D. J. Twitchen, L. Childress, and R. Hanson, Heralded entanglement between solid-state qubits separated by three metres, Nature **497**, 86 (2013).
[38] P. C. Humphreys, N. Kalb, J. P. J. Morits, R. N. Schouten, R. F. L. Vermeulen, D. J. Twitchen, M. Markham, and R. Hanson, Deterministic delivery of remote entanglement on a quantum network, Nature **558**, 268 (2018).
[39] J. M. Kindem, A. Ruskuc, J. G. Bartholomew, J. Rochman, Y. Q. Huan, and A. Faraon, Control and single-shot readout of an ion embedded in a nanophotonic cavity, Nature **580**, 201 (2020).
[40] M. K. Bhaskar, R. Riedinger, B. Machielse, D. S. Levonian, C. T. Nguyen, E. N. Knall, H. Park, D. Englund, M. Lončar, D. D. Sukachev, and M. D. Lukin, Experimental demonstration of memory-enhanced quantum communication, Nature **580**, 60 (2020).
[41] M. T. Uysal, Ł. Dusanowski, H. Xu, S. P. Horvath, S. Ourari, R. J. Cava, N. P. de Leon, and J. D. Thompson, Spin-photon entanglement of a single Er^{3+} ion in the telecom band, Phys. Rev. X **15**, 011071 (2025).
[42] J. W. Lis, A. Senoo, W. F. McGrew, F. Rönchen, A. Jenkins, and A. M. Kaufman, Midcircuit operations using the omg architecture in neutral atom arrays, Phys. Rev. X **13**, 041035 (2023).
[43] S. Ma, G. Liu, P. Peng, B. Zhang, S. Jandura, J. Claes, A. P. Burgers, G. Pupillo, S. Puri, and J. D. Thompson, High-fidelity gates and mid-circuit erasure conversion in an atomic qubit, Nature **622**, 279 (2023).
[44] J. A. Muniz, M. Stone, D. T. Stack, M. Jaffe, J. M. Kindem, L. Wadleigh, E. Zalys-Geller, X. Zhang, C.-A. Chen,

M. A. Norci *et al.*, High-fidelity universal gates in the ^{171}Yb ground-state nuclear-spin qubit, PRX Quantum **6**, 020334 (2025).

[45] M. Peper, Y. Li, D. Y. Knapp, M. Bileska, S. Ma, G. Liu, P. Peng, B. Zhang, S. P. Horvath, A. P. Burgers, and J. D. Thompson, Spectroscopy and modeling of Rydberg states for high-fidelity two-qubit gates, Phys. Rev X **15**, 011009 (2025).

[46] R. Finkelstein, R. B.-S. Tsai, X. Sun, P. Scholl, S. Direkci, T. Gefen, J. Choi, A. L. Shaw, and M. Endres, Universal quantum operations and ancilla-based read-out for tweezer clocks, Nature **634**, 321 (2024).

[47] A. W. Young, W. J. Eckner, W. R. Milner, D. Kedar, M. A. Norcia, E. Oelker, N. Schine, J. Ye, and A. M. Kaufman, Half-minute-scale atomic coherence and high relative stability in a tweezer clock, Nature **588**, 408 (2020).

[48] T. Bothwell, C. J. Kennedy, A. Aeppli, D. Kedar, J. M. Robinson, E. Oelker, A. Staron, and J. Ye, Resolving the gravitational redshift across a millimetre-scale atomic sample, Nature **602**, 420 (2022).

[49] N. Schine, A. W. Young, W. J. Eckner, M. J. Martin, and A. M. Kaufman, Long-lived Bell states in an array of optical clock qubits, Nat. Phys. **18**, 1067 (2022).

[50] A. Cao, W. J. Eckner, T. Lukin Yelin, A. W. Young, S. Jandura, L. Yan, K. Kim, G. Pupillo, J. Ye, N. Darkwah Oppong, and A. M. Kaufman, Multi-qubit gates and Schrödinger cat states in an optical clock, Nature **634**, 315 (2024).

[51] N. D. Lemke, Ph.D. thesis, Graduate School of the University of Colorado-Boulder, 2012.

[52] N. Chen, L. Li, W. Huie, M. Zhao, I. Vetter, C. H. Greene, and J. P. Covey, Analyzing the Rydberg-based optical-metastable-ground architecture for ^{171}Yb nuclear spins, Phys. Rev. A **105**, 052438 (2022).

[53] W. Huie, L. Li, N. Chen, X. Hu, Z. Jia, W. K. C. Sun, and J. P. Covey, Repetitive readout and real-time control of nuclear spin qubits in ^{171}Yb atoms, PRX Quantum **4**, 030337 (2023).

[54] M. A. Norcia *et al.*, Midcircuit qubit measurement and rearrangement in a ^{171}Yb atomic array, Phys. Rev. X **13**, 041034 (2023).

[55] Z. Jia, W. Huie, L. Li, W. K. C. Sun, X. Hu, Aakash, H. Kogan, A. Karve, J. Y. Lee, and J. P. Covey, An architecture for two-qubit encoding in neutral ytterbium-171 atoms, npj Quantum Inf. **10**, 106 (2024).

[56] L.-S. Ma, P. Jungner, J. Ye, and J. L. Hall, Delivering the same optical frequency at two places: Accurate cancellation of phase noise introduced by an optical fiber or other time-varying path, Opt. Lett. **19**, 1777 (1994).

[57] M. Pizzocaro *et al.*, Intercontinental comparison of optical atomic clocks through very long baseline interferometry, Nat. Phys. **17**, 223 (2021).

[58] D. R. Gozzard, L. A. Howard, B. P. Dix-Matthews, S. F. E. Karpathakis, C. T. Gravestock, and S. W. Schediwy, Ultrastable free-space laser links for a global network of optical atomic clocks, Phys. Rev. Lett. **128**, 020801 (2022).

[59] A. D. Ludlow, M. M. Boyd, J. Ye, E. Peik, and P. O. Schmidt, Optical atomic clocks, Rev. Mod. Phys. **87**, 637 (2015).

[60] P. Wcisło *et al.*, New bounds on dark matter coupling from a global network of optical atomic clocks, Sci. Adv. **4**, eaau4869 (2018).

[61] K. Singh, C. E. Bradley, S. Anand, V. Ramesh, R. White, and H. Bernien, Mid-circuit correction of correlated phase errors using an array of spectator qubits, Science **380**, 1265 (2023).

[62] P. Asenbaum, C. Overstreet, T. Kovachy, D. D. Brown, J. M. Hogan, and M. A. Kasevich, Phase shift in an atom interferometer due to spacetime curvature across its wave function, Phys. Rev. Lett. **118**, 183602 (2017).

[63] R. Penrose, On gravity's role in quantum state reduction, Gen. Relativ. Gravit. **28**, 581 (1996).

[64] J. D. Bekenstein, Can quantum gravity be exposed in the laboratory? Found. Phys. **44**, 452 (2014).

[65] T. Ralph and J. Pienaar, Entanglement decoherence in a gravitational well according to the event formalism, New J. Phys. **16**, 085008 (2014).

[66] E. Rydving, E. Aurell, and I. Pikovski, Do Gedanken experiments compel quantization of gravity? Phys. Rev. D **104**, 086024 (2021).

[67] P. Xu, Y. Ma, J.-G. Ren, H.-L. Yong, T. C. Ralph, S.-K. Liao, J. Yin, W.-Y. Liu, W.-Q. Cai, X. Han, *et al.*, Satellite testing of a gravitationally induced quantum decoherence model, Science **366**, 132 (2019).

[68] M. M. Marchese, M. Plávala, M. Kleinmann, and S. Nimmrichter, Newton's laws of motion can generate gravity-mediated entanglement, arXiv:2401.07832.

[69] M. Plávala, S. Nimmrichter, and M. Kleinmann, Probing the nonclassical dynamics of a quantum particle in a gravitational field, arXiv:2502.03489.

[70] R. D. Sorkin, Quantum mechanics as quantum measure theory, Mod. Phys. Lett. A **9**, 3119 (1994).

[71] U. Sinha, C. Couteau, T. Jennewein, R. Laflamme, and G. Weihs, Ruling out multi-order interference in quantum mechanics, Science **329**, 418 (2010).

[72] D. K. Park, O. Moussa, and R. Laflamme, Three path interference using nuclear magnetic resonance: A test of the consistency of Born's rule, New J. Phys. **14**, 113025 (2012).

[73] P. Berglund, T. Hübsch, D. Mattingly, and D. Minic, Gravitizing the quantum, Int. J. Mod. Phys. D **31**, 2242024 (2022).

[74] A. Valentini, Beyond the Born rule in quantum gravity, Found. Phys. **53**, 6 (2023).

[75] P. Berglund, A. Geraci, T. Hübsch, D. Mattingly, and D. Minic, Triple interference, non-linear Talbot effect and gravitization of the quantum, Class. Quantum Grav. **40**, 155008 (2023).

[76] P. Berglund, A. Geraci, T. Hubsch, D. Mattingly, and D. Minic, Information metrics and possible limitations of local information objectivity in quantum gravity, arXiv:2501.19269.

[77] T. M. Graham *et al.*, Multi-qubit entanglement and algorithms on a neutral-atom quantum computer, Nature **604**, 457 (2022).

[78] D. Bluvstein, H. Levine, G. Semeghini, T. T. Wang, S. Ebadi, M. Kalinowski, A. Keesling, N. Maskara, H. Pichler, M. Greiner, V. Vuletić, and M. D. Lukin, A quantum processor based on coherent transport of entangled atom arrays, Nature **604**, 451 (2022).

[79] M. Ringbauer, M. Meth, L. Postler, R. Stricker, R. Blatt, P. Schindler, and T. Monz, A universal qudit quantum processor with trapped ions, Nat. Phys. **18**, 1053 (2022).

[80] S. J. Evered, D. Bluvstein, M. Kalinowski, S. Ebadi, T. Manovitz, H. Zhou, S. H. Li, A. A. Geim, T. T. Wang, N. Maskara, H. Levine, G. Semeghini, M. Greiner, V. Vuletić, and M. D. Lukin, High-fidelity parallel entangling gates on a neutral-atom quantum computer, Nature **622**, 268 (2023).

[81] A. G. Radnaev *et al.*, A universal neutral-atom quantum computer with individual optical addressing and nondestructive readout, arXiv:2408.08288.